

# Making Sense of the Diverse Ligand Recognition by NKG2D<sup>1</sup>

Sergei Radaev,\* Michael Kattah,\* Zhongcheng Zou,\* Marco Colonna,<sup>†</sup> and Peter D. Sun<sup>2\*</sup>

**NKG2D recognizes multiple diverse ligands. Despite recent efforts in determining the crystal structures of NKG2D-ligand complexes, the principle governing this receptor-ligand recognition and hence the criteria for identifying unknown ligands of NKG2D remain central issues to be resolved. Here we compared the molecular recognition between NKG2D and three of the known ligands, UL16 binding protein (ULBP), MHC class I-like molecule, and retinoic acid early inducible gene as observed in the ligand-complexed crystal structures. The comparison shows that while the receptor uses a common interface region to bind the three diverse ligands, each ligand forms a distinct, but overlapping, set of hydrogen bonds, hydrophobic interactions, and salt bridges, illustrating the underlying principle of NKG2D-ligand recognition being the conservation in overall shape complementarity and binding energy while permitting variation in ligand sequence through induced fit recognition. To further test this hypothesis and to distinguish between diverse recognition and promiscuous ligand binding, four ULBP3 interface mutations, H21A, E76A, R82M, and D169A, were generated to each disrupt a single hydrogen bond or salt bridge. All mutant ULBP3 displayed reduced receptor binding, suggesting a specific, rather than promiscuous, receptor-ligand recognition. Mutants with severe loss of binding affect the receptor interactions that are mostly buried. Finally, a receptor-ligand recognition algorithm was developed to assist the identification of diverse NKG2D ligands based on evaluating the potential hydrogen bonds, hydrophobic interactions, and salt bridges at the receptor-ligand interface. *The Journal of Immunology*, 2002, 169: 6279–6285.**

**T**he cytolytic activity of NK cells depends upon the balance between their surface-expressing activating and inhibitory receptors (1–5). While the inhibitory receptors, such as killer Ig receptor (KIR),<sup>3</sup> Ig-like transcript (ILT), CD94/NKG2, and some Ly49 receptors, possess ITIM motifs in their cytoplasmic tail, the activating NK receptors carry a transmembrane charge to couple with either ITAM-containing FcR $\gamma$ , CD3 $\xi$ , and DNAX activation protein (DAP)12 or ITAM-less DAP10 adaptor molecules. In human, examples of known activating NK receptors include NKR-P1, CD16, 2B4, NKG2D, NKp46, NKp30, and NKp44. In mice, certain Ly49 receptors, such as Ly49D and Ly49H, are also part of the activating NK receptors. To date, the ligands for many inhibitory receptors have been identified as self-class I MHC molecules. Crystal structures of three inhibitory receptor-ligand complexes, the KIR2DL2/HLA-Cw3 and KIR2DL1/HLA-Cw4 in humans and the Ly49A/H-2D<sup>d</sup> in mice (6–8), revealed molecular recognition between the inhibitory receptors and their cognate class I MHC ligands.

In contrast, the ligands for many activating receptors, with exception of 2B4, NKG2D, and Ly49H, remain to be identified. The

ligands for NKG2D, an activating receptor that signals through DAP10 and phosphoinositol 3-kinase, have been identified as class I MHC-like families of MIC and ULBP proteins in humans and as H60 and retinoic acid early inducible gene (Rae1) proteins in mice (9–12). The expression of these genes has been shown on the surface of certain tumor cells or to be stress induced. Unlike the inhibitory KIR that recognize a set of conserved residues in the polymorphic region of classical MHC molecules and are capable of distinguishing class I MHC ligands based on single amino acid changes (6, 13, 14), NKG2D recognizes diverse ligands with not only limited sequence homology (25–40% sequence identities between the families), but also different domain organizations. For example, while all NKG2D ligands possess the homologous class I MHC-like  $\alpha$ 1 and  $\alpha$ 2 domains, MIC genes contain additional  $\alpha$ 3 and transmembrane domains, whereas ULBP, Rae1, and H60 families are glycosylphosphatidylinositol anchored.

To understand the principle of NKG2D ligand recognition, the crystal structures of a murine ligand-free NKG2D and its complex with Rae1 $\beta$  (15, 16), the human NKG2D/MHC class I-like molecule (MICA) and NKG2D/ULBP3 complexes (17, 18), have been determined. The results show that while the overall docking between NKG2D and the ligands is similar, the detailed receptor-ligand interfaces vary considerably among the MICA, ULBP3 and Rae1 $\beta$  complexed structures. First, aside from a small number of conserved hydrogen bonds and salt bridges, more than half the ligand interface residues vary either in their amino acid identities or in their location. Second, despite a common set of NKG2D residues found in the interface of all three ligand complexes, a number of these interface residues adopt distinct side chain conformations and interact with different ligand residues in different complexes. This led to an induced fit hypothesis for NKG2D-ligand recognition, in which the local conformation of the receptor is dictated in part by the constitution of its ligand interface residues (18). The plastic nature of the NKG2D-ligand interface is consistent with the ability of the receptor to recognize diverse ligands. The basis for this interface plasticity, the principle of NKG2D recognition, however, is still unclear.

\*Structural Immunology Section, Laboratory of Immunogenetics, National Institute of Allergy and Infectious Diseases, National Institutes of Health, Rockville, MD 20852; and <sup>†</sup>Department of Pathology and Immunology, Washington University School of Medicine, St. Louis, Missouri 63110

Received for publication June 20, 2002. Accepted for publication October 1, 2002.

The costs of publication of this article were defrayed in part by the payment of page charges. This article must therefore be hereby marked *advertisement* in accordance with 18 U.S.C. Section 1734 solely to indicate this fact.

<sup>1</sup> This work was supported by the intramural research funding from the National Institute of Allergy and Infectious Diseases, National Institutes of Health.

<sup>2</sup> Address correspondence and reprint requests to Dr. Peter D. Sun, Structural Immunology Section, Laboratory of Immunogenetics, National Institute of Allergy and Infectious Diseases, National Institutes of Health, 12441 Parklawn Drive, Rockville, MD 20852. E-mail: psun@nih.gov

<sup>3</sup> Abbreviations used in this paper: KIR, killer Ig receptor; ILT, Ig-like transcript; ITAM, immunotyrosine-containing activation motif; ITIM, immunotyrosine-containing inhibitory motif; MICA, MHC class I-like molecule; PDB, Protein Data Bank; Rae1, retinoic acid early inducible gene; r.m.s., root-mean-square; ULBP, UL16 binding protein; DAP, DNAX activation protein.

Table I. Oligonucleotide primers used for generating ULBP3 mutants

Primers	Sequences
Common primers	
5' primer	TAGTAGCATATGGACTGGTCCGGGACGGGGCGGG
3' primer	TAGTAGCTCGAGTTTGGGTTGAGCTAAGCCTGGGG
Mutant-specific primers	
H21A	
R <sup>a</sup>	CCCATGTCTGGGCAAGCAATGATGGTGAAGTT
F <sup>b</sup>	AACTTCACCATCATTGCTTTGCCAGACATGGG
E76A	
R	GAGCCTCTGCCCCACCGCTCTCAGCATTTCAG
F	CTGGAAATGCTGAGAGCGGTGGGGCAGAGGCTC
R82M	
R	GTCAGCCAGTTCAGCATGAGCCTCTGCCCCAC
F	GTGGGGCAGAGGCTCATGCTGGAAGTGGCTGAC
D169A	
R	AAGCCAGCTCTTGCCAGGCTCTCATTGAGACCAT
F	ATGGTCTCAATGAGAGCCTGCAAGAGCTGGCTT

<sup>a</sup> R, Reverse primer for 5' fragment.<sup>b</sup> F, Forward primer for 3' fragment.

Through structural comparison between the receptor-ligand complexes and through mutational studies that affect NKG2D/ULBP3 binding, we attempted to address factors important for this receptor-ligand recognition. In doing so, we hoped not only to understand the underlying principle of NKG2D-ligand recognition, but more importantly to predict unknown ligands of the receptor.

## Materials and Methods

### Protein Data Bank (PDB) coordinates and structural analysis

The PDB accession codes for the structures of murine NKG2D, MICA, Rae1 $\beta$ , and NKG2D/MICA, NKG2D/ULBP3, NKG2D/Rae1 $\beta$  complexes are 1HQ8, 1B3J, 1JFM, 1HYR, 1KCG, and 1JSK, respectively. The PDB accession codes for the structures of KIR2DL2/HLA-Cw3, neonatal FcR, hereditary hemochromatosis protein are 1FEX, 1EXU, and 1DE4, respectively. All structural superposition analyses were performed using the program LSQMAN (19), and domain orientations were calculated with program HINGE (20).

### Recombinant constructs for ULBP3 mutants

The cDNA encoding the extracellular region of ULBP3 was cloned into pET22b (Novagen, San Diego, CA) as previously described (18). For each mutant, the 5' and 3' overlapping fragments of ULBP3 were amplified from ULBP3-pET22b in separate PCRs. The forward primer for the 5' fragments and the reverse primer for the 3' fragments were identical for all mutants and contained an *NdeI* and an *XhoI* restriction site, respectively (Table I). The reverse primer for the 5' fragment and the forward primer for the 3' fragment were complementary and included the nucleotide substitution generating the amino acid variation (Table I). Amplified 5' and 3' fragment pairs of each mutant were purified by agarose gel electrophoresis, mixed, and reamplified using the common forward and reverse primers. Amplified fragments were purified by agarose gel electrophoresis, digested

with *NdeI* and *XhoI*, and cloned into the corresponding sites of pET22b. Incorporation of the appropriate nucleotide substitution in each ULBP3 mutant was confirmed by DNA sequencing.

### Protein expression and purification

The mutants of ULBP3 (residues 1–200) were expressed as *Escherichia coli* inclusion bodies and then reconstituted in vitro. In brief, cells containing ULBP3-expressing plasmid were grown in a 10 L Bioflo 3000 bioreactor vessel (New Brunswick Scientific, Edison, NJ) and induced with 0.5 mM isopropyl- $\beta$ -D-thiogalactopyranoside at an approximate OD<sub>596</sub> of 1.7 for 4 h. The inclusion bodies were isolated by washing repeatedly with a 2 M urea solution and then were dissolved in 6 N guanidine hydrochloride before refolding. The refolding buffer consisted of 0.5 M L-arginine, 2.5 mM cystamine (or oxidized glutathione), 5 mM cysteamine (or reduced glutathione), 10  $\mu$ g/ml AEBSF, and 100 mM Tris (pH 8.0). The renatured ULBP3 was concentrated on a nickel affinity column (Qiagen, Chatsworth, CA) and was further purified on a Superdex 200 size exclusion column (Amersham Pharmacia Biotech, Piscataway, NJ). All mutations were confirmed by electrospray ionization mass spectrometry.

### Surface plasmon resonance measurements

Surface plasmon resonance measurements were performed using BIAcore 3000 instrument (BIAcore, Piscataway, NJ). The receptor, NKG2D, was immobilized at a concentration of 1  $\mu$ M in 10 mM sodium acetate, pH 5.2, on a CM5 sensor chip using *N*-hydroxysuccinimide/1-ethyl-3-(3-dimethylaminopropyl)-carbodiimide hydrochloride at a flow rate of 20  $\mu$ l/min. Flow cell 1 was mocked with *N*-hydroxysuccinimide/1-ethyl-3-(3-dimethylaminopropyl)-carbodiimide hydrochloride. The binding buffer consisted of 20 mM NaCl, 3 mM EDTA, 0.005% surfactant P20, and 10 mM HEPES, pH 7.4, mixed with various concentrations of analyte. Binding of the wild-type and mutant ULBP3 proteins to immobilized NKG2D was measured using serial dilutions of the analyte from 30 to 0.059  $\mu$ M at a flow rate of 20  $\mu$ l/min. All  $K_d$  were obtained either from a linear regression of steady state 1/response vs 1/C plots using ORIGIN 3.0 (OriginLab, Northampton, MA) or from kinetic rate constants fitted with the BIAevaluation software package (BIAcore).

## Results and Discussion

### NKG2D is more conserved than its ligands

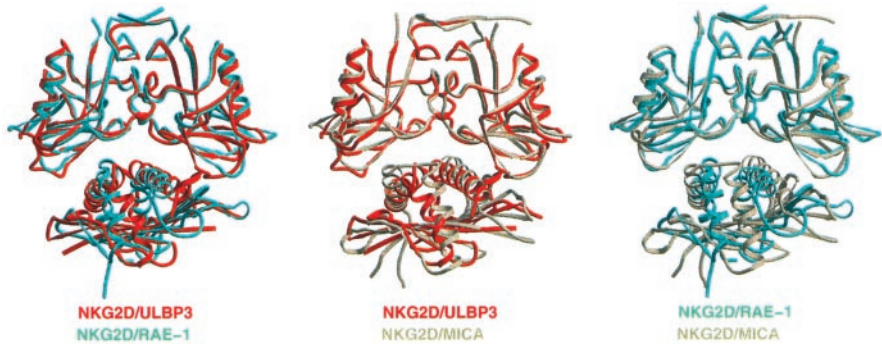
NKG2D displays significant conservation at both the amino acid sequence and the three-dimensional structural level. The overall sequence identity of the receptor is ~60% between human and mouse. At the structural level, the superposition between the human and murine NKG2D results in a root-mean-square (r.m.s.) deviation of 0.95 Å among 233 C $\alpha$  atoms. In contrast, the amino acid sequences of NKG2D ligands share <40% identity between the human ULBP and mouse Rae1 genes (Table II). The divergence in amino acid sequence is also reflected at the level of three-dimensional structures (Table II). The superposition of the  $\alpha$ 1 and  $\alpha$ 2 domains between the human and mouse ligands resulted in an r.m.s. deviation of 2.3 Å, considerably worse than the structural agreement between the human and mouse NKG2D.

Table II. Structure and sequence diversity between NKG2D and its ligands

	hNKG2D	mNKG2D		r.m.s. Structural Differences <sup>a</sup>					
				ULBP3	Rae1 $\beta$	MICA	HLA-Cw3	HFE	FcRn
hNKG2D	0	0.95	ULBP3	0	2.3	2.4	2.7	1.8	2.7
mNKG2D	60	0	Rae1 $\beta$	24	0	3.9	3.4	3.2	3.4
			MICA	28	20	0	2.7	2.6	3.3
			HLA-Cw3	23	20	32	0	1.7	2.8
			HFE	25	20	31	38	0	1.9
			FcRn	25	23	27	32	30	0

<sup>a</sup> The r.m.s. structural difference is calculated between the positional coordinates (x, y, z) for corresponding C $\alpha$  atoms of two superimposed structures. The numbers above the diagonal of the matrix are the r.m.s. deviations between the crystal structures in angstroms, and the numbers below the diagonal of the matrix are the percent amino acid sequence identities. Approximately the same numbers of C $\alpha$  atoms (~144 pairs) that correspond to their respective regions of structure are used in the structural superposition between the NKG2D ligands.

**FIGURE 1.** Structural overlay of NKG2D/ULBP3 (red), NKG2D/MICA (beige), and NKG2D/Rae1 $\beta$  (green) complexes



*NKG2D-ligand docking mode is dictated by overall shape complementarity*

Interface complementarity between two interacting protein surfaces is often measured by a shape complementarity index, *Sc*, which calculates the surface topology of two interacting proteins and measures the degree of complementarity in their interacting surfaces by a curvature analysis. *Sc* values range from 0–1, with 0 being noncomplementary and 1 being a complete surface match (21). The *Sc* values for highly complementary interfaces, such as those between proteases and protease inhibitors and between Abs and Ags, are in the range of 0.65–0.75 (21). The less complementary interfaces, such as those between TCRs and their class I MHC ligands, have *Sc* values between 0.45 and 0.6 (22). The calculated *Sc* values for the three NKG2D complexed structures are 0.72, 0.65, and 0.63, for the MICA, ULBP3 and Rae1 $\beta$  complexes respectively (16–18). These values are also greater than those between KIR and HLA (*Sc* = 0.58) (6) and between CD2 and CD58 (*Sc* = 0.58) (23), indicating a good shape complementarity in NKG2D-ligand recognition. Despite the diverse ligand sequences, all three NKG2D-ligand complex structures display similar overall receptor-ligand binding (Fig. 1). In particular, the receptor in all three complexes uses a common set of residues to interface with the ligand residues in common structural regions. This conservation in receptor binding mode among the diverse ligands suggests the importance of shape complementarity in NKG2D-ligand recognition.

*NKG2D ligands match the receptor interface hydrogen bonds and hydrophobic requirement with their distinct residues*

The question of what mechanism NKG2D receptor employs to recognize very diverse ligands can be addressed by a detailed structural comparison of binding modes in three different NKG2D receptor-ligand complexes known to date. First, there are no large conformational changes in either the receptor or the ligands upon

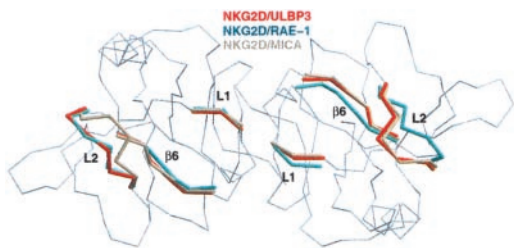


**FIGURE 2.** Structural comparison of NKG2D secondary structure elements involved in the ligand binding. Loops L1 and L2 and the  $\beta 6$  strand are shown as a thick colored lines. Secondary structure elements of NKG2D from its complex with ULBP3 are colored red, those from MICA complex are beige, and those from Rae1 $\beta$  complex are green, respectively. The overall trace of NKG2D is given as a thin gray line for reference.

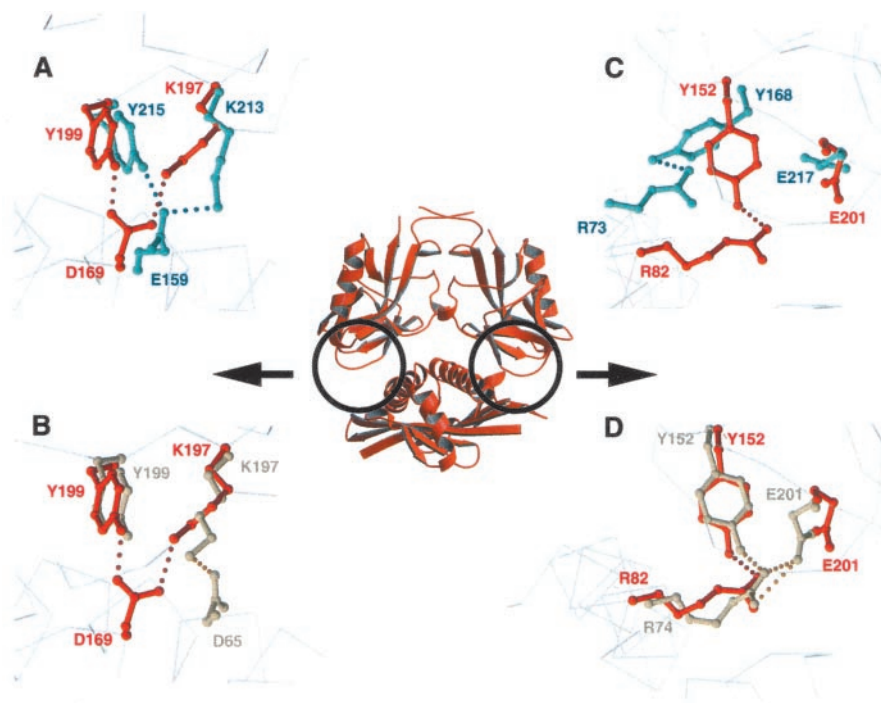
complex formation. This is evident from an r.m.s. deviation of 0.48 Å (among 246 C $\alpha$  atoms) between the structure of a murine ligand-free and that of the Rae1 $\beta$ -bound NKG2D, and the r.m.s. differences of 0.92 Å (for 147 C $\alpha$  pairs) and 0.57 Å (for 147 C $\alpha$  pairs) between the structures of receptor-free and receptor-bound ligands for MICA and Rae1 $\beta$ , respectively. Second, variations in docking orientation are observed in each structure to compensate

Table III. List of NKG2D-ligand interface interactions

NKG2D	ULBP3	MICA	Rae1 $\beta$
Hydrogen bonds <sup>a</sup>			
K150 A		A150	E148
T180 A	K69		
I181 A		Q166	
M184 A	K171		
Q185 A		H158	
S195 A	E72	R64	
<u>Y199 A</u>	D169	D163	E159
I200 A	R168		
N207 A		T155	K151
S151 B	Q79		
<u>Y152 B</u>	R82	R74	R73
E183 B	H21	K81	
Q185 B		V18	
M184 B	H21		
K186 B		D15, S17	P16
K197 B			N78
Y199 B		H79	N74
T205 B		S20	
N207 B		R38	
Total no. 19	9	13	7
Salt bridges			
E183 A	K171		
<u>K197 A</u>	D169	D65	E159
K150 B	E76		
E201 B		R74	
K197 B		D149	
Total no. 5	3	3	1
Hydrophobic contacts			
Cluster A			
Y152 A	M164	A159	F155
I182 A	R168	A162, Q166	
M184 A	R168	H158, A162	H158
L191		T155	
Y199 A	M164, R168	A159	F155
Cluster B			
Y152 B	Q79, L83	M75	W21
I182	A86, D87	H79	
M184	H21, R82, A86	V18, R74, A78	P14
Q185	P23		
A193	L83		
Y199	L83	M75	R73

<sup>a</sup> Hydrogen bonds and salt bridges that are conserved among the three ligands are underlined.

**FIGURE 3.** Conformational plasticity in NKG2D/ligand interactions. *A* and *B*, and *C* and *D* show a zoomed-in interface area between subunit A of NKG2D and a ligand and subunit B of NKG2D and a ligand, respectively. Only interactions made by conserved ligand residues are presented. An image of the NKG2D/ULBP3 complex in the center is given for the orientation. Side chains from NKG2D/ULBP3, NKG2D/MICA, and NKG2D/Rae1 $\beta$  complexes are shown in red, beige, and green, respectively. Hydrogen bonds and salt bridges are presented as dotted lines, colored according to the respective complex



for individual ligand surfaces. When the three complex structures are superimposed using only their NKG2D subunits, the three ligand orientations vary slightly from each other by  $\sim 6^\circ$  (rotation required to superimpose the ligands) between ULBP3 and MICA,  $10^\circ$  between ULBP3 and Rae1 $\beta$ , and  $10^\circ$  between MICA and Rae1 $\beta$ . Thus, it appears that NKG2D accommodates diverse ligand surfaces through adjustments in their docking orientations. Third, variations in loop and side chain conformations are observed in both the receptor and the ligands to reflect their diverse interfaces. On the receptor side, the conformation of the L2 loop, residues 181–185 on both subunits of the receptor dimer, varies  $\sim 4$ – $5$  Å in position among the three complexes (Fig. 2). There are  $\sim 23$  NKG2D residues, half from each subunit, at the ligand interface area. Most of them are identical between human and mouse. They form a total of 19 hydrogen bonds, five salt bridges, and two hydrophobic clusters (Table III). Among them, only two hydrogen bonds (1) from aspartate or glutamate of a ligand to Tyr<sup>199</sup> of the receptor and 2) from arginine of a ligand to Tyr<sup>152</sup> of the receptor) and one salt bridge between aspartic or glutamic acid of a ligand and Lys<sup>197</sup> of the receptor are conserved in all three structures. While different ligands form different hydrogen bonds with NKG2D, about half of the hydrogen bonds are common between any two of the ligands. For example, four hydrogen bonding NKG2D residues Ser<sup>195</sup>, Tyr<sup>199</sup>, Tyr<sup>152</sup>, and Glu<sup>183</sup> are common between the ULBP3 and MICA complexes. Similarly, a subset of

distinct, but overlapping, NKG2D residues participates in hydrophobic interactions with each of the ligands.

On the ligand side, alternative side chain pairing and conformations are also observed for the interface residues (18). MICA, ULBP3, and Rae1 $\beta$  each contribute 25, 19, and 17 residues, respectively, to the receptor interface. Among them, eight residues share common sequence positions, and only two residues, Arg<sup>82</sup> and Asp<sup>169</sup> (ULBP3 numbering), are conserved. However, conformational and sequence variations are also observed even for these relatively conserved residues. For example, Asp<sup>169</sup>, conserved between MICA and ULBP3, but replaced by Glu in Rae1 $\beta$ , forms a hydrogen bond with Tyr<sup>199</sup> of NKG2D in all three structures (Fig. 3, *A* and *B*). It also forms a salt bridge with Lys<sup>197</sup> of NKG2D in ULBP3 and Rae1 $\beta$  complexes, but in the MICA complex, Lys<sup>197</sup> forms a salt bridge with a different aspartate residue, Asp<sup>65</sup>. The other conserved residue, Arg<sup>82</sup> of ULBP3, forms a hydrogen bond with Tyr<sup>152</sup> of NKG2D. This Arg-Tyr pair has a similar side conformation in both the ULBP3 and MICA complexes, except the arginine of MICA makes an additional salt bridge with Glu<sup>201</sup> of the receptor (Fig. 3*D*). The same Arg-Tyr pair, however, interacts differently in the Rae1 $\beta$  complex, in which Tyr<sup>152</sup> adopts an alternative side chain conformation and the arginine is located  $\sim 5$  Å away from Arg<sup>82</sup> of ULBP3 (Fig. 3*C*). Aside from the conserved residues, each ligand appears to form a set of distinct, but overlapping, hydrogen bonds with NKG2D (Fig.

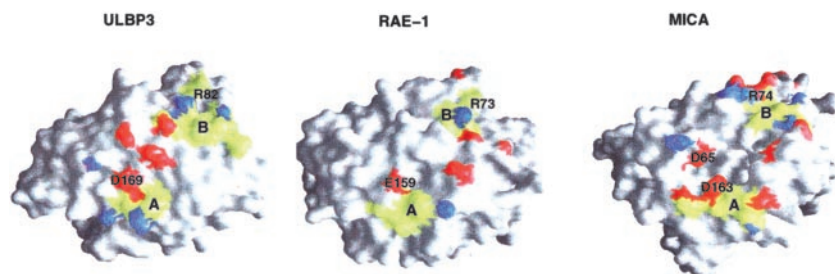


**FIGURE 4.** Surface representation of NKG2D ligands. Hydrophobic residues involved in interactions with the receptor are shown in yellow; positive and negative charges are painted blue and red, respectively. In this view of ligands, the groove between the  $\alpha 1$  and  $\alpha 2$  helices is oriented horizontally across the page.

4 and Table III). The numbers of hydrogen bonds formed between the receptor and MICA, ULBP3, and Rael $\beta$  are 13, nine, and seven, respectively. Similarly, all three ligands appear to form hydrophobic interactions with both clusters A and B of NKG2D, although the shape of each hydrophobic patch varies among the ligands (Fig. 4 and Table III).

Thus, despite the lack of sequence conservation, the ligands of NKG2D appear to have satisfied the receptor interface energetic requirement by forming hydrogen bonds, salt bridges, and hydrophobic interactions using different interface residues. In general, sequence conservation in ligands ensures the preservation of both the free energy of binding at a receptor-ligand interface and the exact local interface residue pairing and hence their conformations between the receptor and its ligand. However, when ligand sequences are not conserved, the preservation of precise local interface receptor-ligand residue pairing becomes difficult. Nevertheless, diverse ligands can still preserve the free energy of binding by making sufficient receptor interface interactions with alternative ligand residues. The receptor in this case is likely to adopt ligand-induced local conformation to best fit the surface of individual ligands.

#### Effect of the ULBP mutations on NKG2D recognition

Four ULBP3 mutations, H21A, E76A, R82M, and D169A, were created in the receptor interface region (Table III), verified both by DNA sequencing of the constructs and by mass spectrometry of the purified inclusion bodies. The refolded mutant proteins display similar m.w. as the wild-type by SDS-PAGE, suggesting that no proteolytic degradation occurred in refolding of the mutants. All

four mutants migrate as monomers similar to the wild-type protein by size exclusion chromatography, indicating no folding defects as the result of mutations (Fig. 5). The binding of the wild-type ULBP3 to NKG2D has a  $K_d$  of 4  $\mu$ M, as measured by BIAcore. The  $K_d$  values for ULBP3 mutants are 30, 105, 233, and 77  $\mu$ M for H21A, E76A, R82M, and D169A, respectively. All mutations resulted in reduced receptor binding affinities compared with the wild type. His<sup>21</sup>, which forms a hydrogen bond with the carbonyl oxygen of Glu<sup>183</sup> of NKG2D, and Glu<sup>76</sup>, which forms a salt bridge with Lys<sup>150</sup> of NKG2D, are not well conserved among the NKG2D ligand sequences. The  $\sim$ 8- and 20-fold reductions in the receptor binding of H21A and E76A mutants indicates that the nonconserved interface hydrogen bond and salt bridge contribute energetically to the receptor recognition. This is consistent with the idea that the ligands of NKG2D need not be conserved in sequence providing they satisfy the receptor interface binding energy requirement. In fact, the mutational loss in binding at Glu<sup>76</sup> is no less than that at Asp<sup>169</sup>, which is quite conserved among the NKG2D ligand sequences. Unexpectedly, R82M is the most destabilizing interface mutation among the four mutations, with  $\sim$ 50-fold reduction in NKG2D binding affinity. This reduction in binding can be attributed largely to the loss of a hydrogen bond between Arg<sup>82</sup> of ULBP3 and Tyr<sup>152</sup> of NKG2D, and the loss of favorable electrostatic interaction between the Arg and Glu<sup>201</sup> of NKG2D, since the Met replacement presumably preserves the hydrophobic interface of the wild-type Arg<sup>82</sup>. It is worth emphasizing that Arg<sup>82</sup> is the most conserved residue among the ligands. It is also nearly

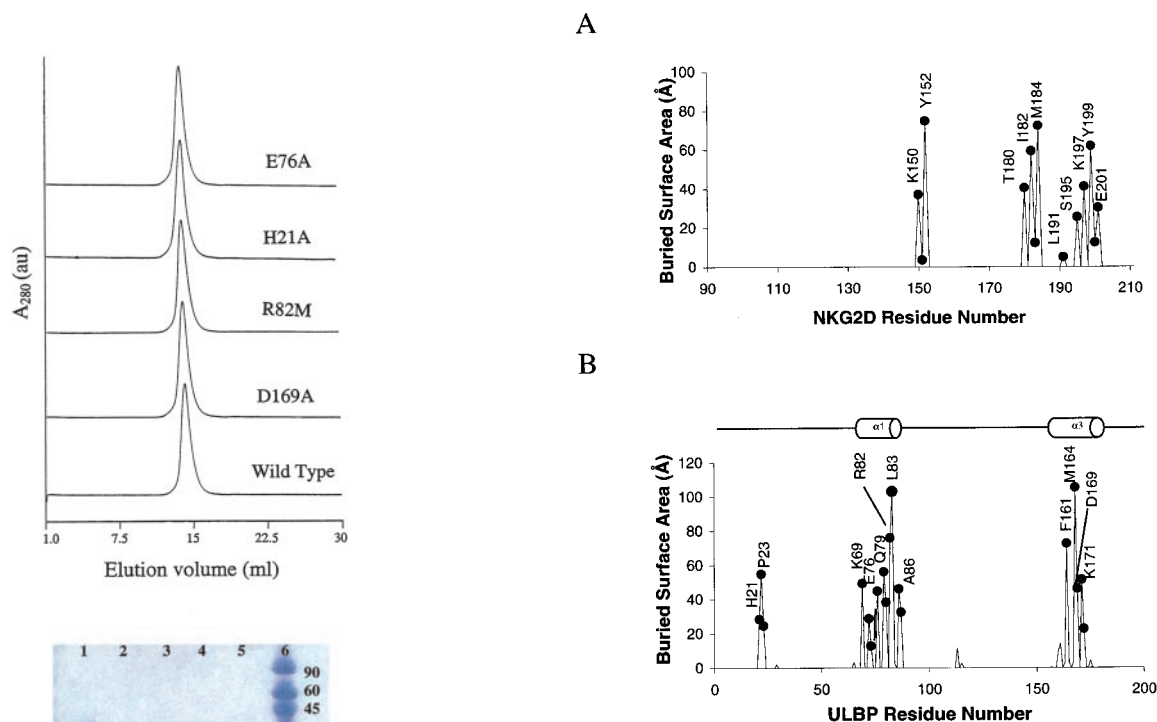


**FIGURE 6.** Plots of the solvent accessible surface area buried upon binding of NKG2D to ULBP3. Solvent accessible surface area values were calculated using the SURFACE program from the CCP4 suite. For each residue, the accessible surface area in the bound state ( $SA_{\text{bound}}$ ) was calculated from the complex crystal structure PDB coordinates (1KCG.pdb). To calculate the accessible surface area for the receptor in the free state ( $SA_{\text{free}}$ ), the PDB coordinates for the ligand were deleted from the complex structure PDB file, and vice versa. The surface area buried was then defined as ( $SA_{\text{free}} - SA_{\text{bound}}$ ). Important interface residues are labeled. Two  $\alpha$  helices of ULBP3 are illustrated as cylinders and are  $\alpha 1$  (65–87) and  $\alpha 3$  (156–183).

**FIGURE 5.** Gel filtration elution profile and SDS-PAGE of ULBP3 mutants. The gel filtration experiments were conducted on an Amersham Bio-science HR10/30 Superdex 200 column. All samples ran at an apparent  $M_r$  of 26 kDa. The sample lanes marked 1–5 are refolded proteins of E76A, H21A, R82M, D169A, and the wild-type ULBP3, respectively. Lane 6, Molecular mass standard (labeled in kilodaltons).

buried at the receptor interface (Fig. 6B). Furthermore, the NKG2D residue that pairs with Arg<sup>82</sup>, namely, Tyr<sup>152</sup>, is among the most buried receptor residues at the interface (Fig. 6A). The drastic reduction in the binding of R82M underscores the importance of the conservation of this residue.

#### Comparison in ligand recognition between NKG2D and inhibitory receptors

To date, the functions of several known inhibitory receptors have been characterized. They include members of KIR family that recognize human classical class I MHC molecules (14, 24, 25), members of the Ly49 family receptors that recognize murine class I MHC molecules (26, 27), the CD94/NKG2 receptors that recognize HLA-E in human and Qa-1 in mouse (28–30), and the ILT/LIR receptors that recognize the  $\alpha 3$  domain of classical class I MHC (31). Compared with NKG2D, the ligand recognition by the inhibitory receptors is quite different. First, the ligands of inhibitory receptors display better structural and sequence conservation than the ligands of NKG2D. At the sequence level all classical class I MHC molecules share >80% sequence identity within species and ~75% sequence identity between human and mouse. Even greater sequence homology is shared among the ligands of individual receptors, such as HLA-Cw allotypes, which are the ligands for KIR2D receptors, sharing >90% sequence identity. Moreover, the receptor-ligand specificities have been shown to be controlled by only a few residues at the ligand side. For example, two amino acids, residues 77 and 80 of the HLA-C heavy chain, are known to control the ligand specificity among the HLA-Cw allotypes for KIR2DL1 and KIR2DL2 receptors (14). Similarly, each inhibitory Ly49 receptor isoform, although often displaying overlapping MHC allelic specificity, generally recognizes a small number of class I MHC alleles (32, 33). The well-recognized sequence conservation among the inhibitory ligands contrasts sharply with the diverse ligands of NKG2D. This creates an interesting receptor-ligand dichotomy. On the one hand, there appear to be too many inhibitory receptors for a family of well-conserved MHC ligands. On the other hand, there are too many diverse ligands for just one NKG2D gene. The question is why the immune system employs multiple, but specific, inhibitory receptors and yet has only one NKG2D.

Second the ligand binding affinities appear to be different between the inhibitory receptors and NKG2D. The affinities between several known inhibitory receptors and their ligands, including that between KIR2D receptors and class I HLA-Cw molecules (6, 34), between Ly49 and their class I MHC ligands, between CD94/NKG2 and HLA-E (35, 36), and between ILT-2 (LIR-1) and class I HLA molecules (37), all have been measured by solution binding experiments to have dissociation constant  $K_d$  of  $\sim 10^{-5}$ – $10^{-6}$  M. This is somewhat lower than the reported  $K_d$  of  $10^{-6}$ – $10^{-8}$  M between NKG2D and its ligands, MICA, H60, and Rae1 (17, 38, 39). The higher affinity of NKG2D is also consistent with the observed larger buried interface area between NKG2D and its ligands (1900–2200 Å<sup>2</sup>) than between KIR and HLA-C's (~1600 Å<sup>2</sup>) (6, 7, 16, 17). The lower affinity of the inhibitory receptors suggests that their ligand binding is closer to the threshold of immune recognition and that they would tolerate less mutational disruptions than NKG2D. Earlier mutational work, in which a single charge to alanine mutations in the receptor resulted in complete loss in ligand recognition, suggested that KIR2DL2/HLA-Cw3 binding was sensitive to mutational changes. Our current results of ULBP3 mutants showed that different mutations resulted in varying degrees of loss in NKG2D binding depending on the site of mutation, suggesting that NKG2D is more tolerant to ligand mutations than KIR.

Third, the structural mechanism of ligand recognition between NKG2D and the inhibitory receptors also appears different. While NKG2D displays significant interface plasticity through induced fit

recognition, the conformation of inhibitory receptors, as shown in the comparison between KIR2DL2/HLA-Cw3 and KIR2DL1/HLA-Cw4 complex structures, remains much the same, indicating a mostly rigid body recognition used by the inhibitory receptors. Since all class I HLA structures differ by 0.6–1 Å in r.m.s. deviations, much smaller than the structural differences among the NKG2D ligands, an induced fit binding mechanism would cause each inhibitory receptor to recognize all class I MHC molecules as ligands. Likewise, if NKG2D adopted a rigid body ligand binding mechanism, it would not be able to recognize the diverse array of ligands. The characteristic rigid body ligand recognition is also consistent with the solution binding data showing very rapid on and off binding kinetics for KIR binding to HLA-C (34) as well as for CD94/NKG2A binding to HLA-E.

The sequence, structural, and mutational data suggest that the immune system employs different ligand recognition mechanisms to best achieve its needs. In the case of inhibitory receptors, whose function is to detect danger through “missing self,” the ligand recognition is very specific, and each receptor is designed to monitor only a small number of conserved class I MHC molecules. In addition, their ligand binding appears to be less tolerant of mutations. The combination of high specificity with low affinity of binding recognition ensures maximum sensitivity in immune surveillance. An immune system is designed not just to recognize a global loss of class I expression as a result of catastrophic events, but also to recognize the disappearance of a few specific class I MHC alleles among otherwise abundant overall surface expression of class I MHC in the event of viral infections. The function of the activating NKG2D receptor is to detect danger through the appearance of stress- or transformation-induced ligands. The diversity in NKG2D ligands presumably reflects complex pathogenic conditions. The combination of a plastic interface with high ligand affinity in NKG2D-ligand recognition ensures maximum efficiency in capturing all possible ligands.

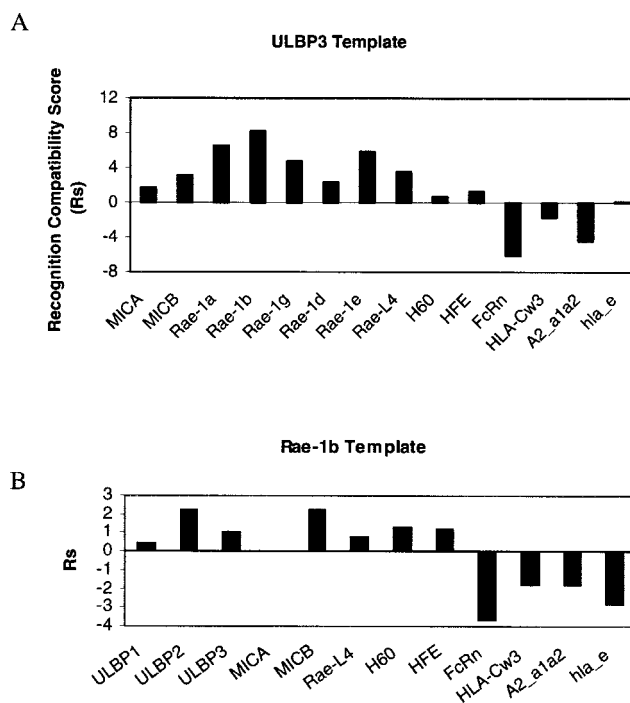


**FIGURE 7.** Recognition compatibility score. *A*, Sequences are scored based on the NKG2D/ULBP3 structural template and are shown as relative scores to HLA-E. *B*, Scores are calculated based on NKG2D/Rae1 $\beta$  template and are shown as relative scores to MICA.

### Evaluating ligands of NKG2D by a recognition compatibility score

Predicting ligands of NKG2D becomes a difficult task due to their lack of sequence and structural conservation. In an attempt to evaluate the unique attributes among these ligands, we have developed a receptor-ligand recognition compatibility score that evaluates potential ligands based on their abilities to form interface salt bridges, hydrogen bonds, and hydrophobic interactions, rather than sequence conservation. The algorithm calculates the solvent accessibility weighted energetic contribution for each interface residues in the structure of a receptor-ligand complex, applies the energy calculation to new sequences to which the structures are not known, and evaluates the compatibility based on a mutational matrix (<http://red.niaid.nih.gov/programs.html>). Using this algorithm, a set of sequences corresponding to both the ligands and nonligands of NKG2D were scored using both NKG2D/ULBP and NKG2D/Rae1 $\beta$  complex structures as templates (Fig. 7). Overall, the NKG2D ligands scored higher than nonligands. In principle, this interface compatibility scoring algorithm should also work for nondiverse ligands in which sequence conservation alone is able to differentiate between the ligands and nonligands of a receptor. To test this, a set of classical class I MHC sequences was scored for their compatibility of being ligands of KIR2DL2. The results show that all ligands of KIR2DL2, including HLA-Cw1, -3, -7, and -8, have a score of 8.6, which is higher than the score of 5.6 for ligands of KIR2DL1. Interestingly, while most HLA-B alleles scored  $\sim$ 3.0, HLA-B46, which is known to bind KIR2DL2 (40), scored 8.6, the same as other KIR2DL2 ligands.

### Acknowledgments

We thank C. Hammer for mass spectroscopy measurements, M. Garfield for N-terminal peptide sequencing, and R. Strong for providing the PDB coordinates of Rae1 and NKG2D/Rae1 complex before publication.

### References

1. Cerwenka, A., and L. L. Lanier. 2001. Ligands for natural killer cell receptors: redundancy or specificity. *Immunol. Rev.* 181:158.
2. Ravetch, J. V., and L. L. Lanier. 2000. Immune inhibitory receptors. *Science* 290:84.
3. Long, E. O. 1999. Regulation of immune responses through inhibitory receptors. *Annu. Rev. Immunol.* 17:875.
4. Smith, H. R., A. H. Idris, and W. M. Yokoyama. 2001. Murine natural killer cell activation receptors. *Immunol. Rev.* 181:115.
5. Diefenbach, A., and D. H. Raulet. 2001. Strategies for target cell recognition by natural killer cells. *Immunol. Rev.* 181:170.
6. Boyington, J. C., S. A. Motyka, P. Schuck, A. G. Brooks, and P. D. Sun. 2000. Crystal structure of an NK cell immunoglobulin-like receptor in complex with its class I MHC ligand. *Nature* 405:537.
7. Fan, Q. R., E. O. Long, and D. C. Wiley. 2001. Crystal structure of the human natural killer cell inhibitory receptor KIR2DL1-HLA-Cw4 complex. *Nat. Immunol.* 2:452.
8. Tormo, J., K. Natarajan, D. H. Margulies, and R. A. Mariuzza. 1999. Crystal structure of a lectin-like natural killer cell receptor bound to its MHC class I ligand. *Nature* 402:623.
9. Bauer, S., V. Groh, J. Wu, A. Steinle, J. H. Phillips, L. L. Lanier, and T. Spies. 1999. Activation of NK cells and T cells by NKG2D, a receptor for stress-inducible MICA. *Science* 285:727.
10. Cosman, D., J. Mullberg, C. L. Sutherland, W. Chin, R. Armitage, W. Fanslow, M. Kubin, and N. J. Chalupny. 2001. ULBPs, novel MHC class I-related molecules, bind to CMV glycoprotein UL16 and stimulate NK cytotoxicity through the NKG2D receptor. *Immunity* 14:123.
11. Cerwenka, A., A. B. Bakker, T. McClanahan, J. Wagner, J. Wu, J. H. Phillips, and L. L. Lanier. 2000. Retinoic acid early inducible genes define a ligand family for the activating NKG2D receptor in mice. *Immunity* 12:721.
12. Diefenbach, A., A. M. Jamieson, S. D. Liu, N. Shastri, and D. H. Raulet. 2000. Ligands for the murine NKG2D receptor: expression by tumor cells and activation of NK cells and macrophages. *Nat. Immunol.* 1:119.
13. Winter, C. C., and E. O. Long. 1997. A single amino acid in the p58 killer cell inhibitory receptor controls the ability of natural killer cells to discriminate between the two groups of HLA-C allotypes. *J. Immunol.* 158:4026.
14. Colonna, M., G. Borsellino, M. Falco, G. B. Ferrara, and J. L. Strominger. 1993. HLA-C is the inhibitory ligand that determines dominant resistance to lysis by NK1- and NK2-specific natural killer cells. *Proc. Natl. Acad. Sci. USA* 90:12000.
15. Wolan, D. W., L. Teyton, M. G. Rudolph, B. Villmow, S. Bauer, D. H. Busch, and I. A. Wilson. 2001. Crystal structure of the murine NK cell-activating receptor NKG2D at 1.95 Å. *Nat. Immunol.* 2:248.
16. Li, P., G. McDermott, and R. K. Strong. 2002. Crystal structures of RAE-1 $\beta$  and its complex with the activating immunoreceptor NKG2D. *Immunity* 16:77.
17. Li, P., D. L. Morris, B. E. Willcox, A. Steinle, T. Spies, and R. K. Strong. 2001. Complex structure of the activating immunoreceptor NKG2D and its MHC class I-like ligand MICA. *Nat. Immunol.* 2:443.
18. Radaev, S., B. Rostro, A. G. Brooks, M. Colonna, and P. D. Sun. 2001. Conformational plasticity revealed by the cocrystal structure of NKG2D and its class I MHC-like ligand ULBP3. *Immunity* 15:1.
19. Kleywegt, G. J., and T. A. Jones. 1995. Where freedom is given, liberties are taken. *Structure* 3:535.
20. Snyder, G. A., A. G. Brooks, and P. D. Sun. 1999. Crystal structure of the HLA-Cw3 allotype-specific killer cell inhibitory receptor KIR2DL2. *Proc. Natl. Acad. Sci. USA* 96:3864.
21. Lawrence, M. C., and P. M. Colman. 1993. Shape complementarity at protein/protein interfaces. *J. Mol. Biol.* 234:946.
22. Ysern, X., H. Li, and R. A. Mariuzza. 1998. Imperfect interfaces. *Nat. Struct. Biol.* 5:412.
23. Wang, J. H., A. Smolyar, K. Tan, J. H. Liu, M. Kim, Z. Y. Sun, G. Wagner, and E. L. Reinherz. 1999. Structure of a heterophilic adhesion complex between the human CD2 and CD58 (LFA-3) counterreceptors. *Cell* 97:791.
24. Wagtmann, N., S. Rajagopalan, C. C. Winter, M. Peruzzi, and E. O. Long. 1995. Killer cell inhibitory receptors specific for HLA-C and HLA-B identified by direct binding and by functional transfer. *Immunity* 3:801.
25. Gumperz, J. E., L. D. Barber, N. M. Valiante, L. Percival, J. H. Phillips, L. L. Lanier, and P. Parham. 1997. Conserved and variable residues within the Bw4 motif of HLA-B make separable contributions to recognition by the NK1 killer cell-inhibitory receptor. *J. Immunol.* 158:5237.
26. Karlhofer, F. M., R. K. Ribaud, and W. M. Yokoyama. 1992. MHC class I alloantigen specificity of Ly-49<sup>+</sup> IL-2-activated natural killer cells. *Nature* 358:66.
27. Yokoyama, W. M. 1998. Natural killer cell receptors. *Curr. Opin. Immunol.* 10:298.
28. Braud, V. M., D. S. Allan, C. A. O'Callaghan, K. Soderstrom, A. D'Andrea, G. S. Ogg, S. Lazetic, N. T. Young, J. I. Bell, J. H. Phillips, et al. 1998. HLA-E binds to natural killer cell receptors CD94/NKG2A, B and C. *Nature* 391:795.
29. Brooks, A. G., F. Borrego, P. E. Posch, A. Patamawenu, C. J. Scorzelli, M. Ulbrecht, E. H. Weiss, and J. E. Coligan. 1999. Specific recognition of HLA-E, but not classical, HLA class I molecules by soluble CD94/NKG2A and NK cells. *J. Immunol.* 162:305.
30. Vance, R. E., J. R. Kraft, J. D. Altman, P. E. Jensen, and D. H. Raulet. 1998. Mouse CD94/NKG2A is a natural killer cell receptor for the nonclassical major histocompatibility complex (MHC) class I molecule Qa-1(b). *J. Exp. Med.* 188:1841.
31. Colonna, M., F. Navarro, T. Bellon, M. Llano, P. Garcia, J. Samaridis, L. Angman, M. Cella, and M. Lopez-Botet. 1997. A common inhibitory receptor for major histocompatibility complex class I molecules on human lymphoid and myelomonocytic cells. *J. Exp. Med.* 186:1809.
32. Anderson, S. K., J. R. Ortaldo, and D. W. McVicar. 2001. The ever-expanding Ly49 gene family: repertoire and signaling. *Immunol. Rev.* 181:79.
33. Hanke, T., H. Takizawa, C. W. McMahon, D. H. Busch, E. G. Pamer, J. D. Miller, J. D. Altman, Y. Liu, D. Cado, F. A. Lemonnier, et al. 1999. Direct assessment of MHC class I binding by seven Ly49 inhibitory NK cell receptors. *Immunity* 11:67.
34. Maenaka, K., T. Juji, T. Nakayama, J. R. Weyer, G. F. Gao, T. Maenaka, N. R. Zaccari, A. Kikuchi, T. Yabe, K. Tokunaga, et al. 1999. Killer cell immunoglobulin receptors and T cell receptors bind peptide-major histocompatibility complex class I with distinct thermodynamic and kinetic properties. *J. Biol. Chem.* 274:28329.
35. Chung, D. H., K. Natarajan, L. F. Boyd, J. Tormo, R. A. Mariuzza, W. M. Yokoyama, and D. H. Margulies. 2000. Mapping the ligand of the NK inhibitory receptor Ly49A on living cells. *J. Immunol.* 165:6922.
36. Vales-Gomez, M., H. T. Reyburn, R. A. Erskine, M. Lopez-Botet, and J. L. Strominger. 1999. Kinetics and peptide dependency of the binding of the inhibitory NK receptor CD94/NKG2-A and the activating receptor CD94/NKG2-C to HLA-E. *EMBO J.* 18:4250.
37. Chapman, T. L., A. P. Heikeman, and P. J. Bjorkman. 1999. The inhibitory receptor LIR-1 uses a common binding interaction to recognize class I MHC molecules and the viral homolog UL18. *Immunity* 11:603.
38. O'Callaghan, C. A., A. Cerwenka, B. E. Willcox, L. L. Lanier, and P. J. Bjorkman. 2001. Molecular competition for NKG2D: H60 and RAE1 compete unequally for NKG2D with dominance of H60. *Immunity* 15:201.
39. Carayannopoulos, L., O. Naidenko, J. Kinder, E. Ho, D. Fremont, and W. Yokoyama. 2002. Ligands for murine NKG2D display heterogeneous binding behavior. *Eur. J. Immunol.* 32:597.
40. Barber, L. D., L. Percival, N. M. Valiante, L. Chen, C. Lee, J. E. Gumperz, J. H. Phillips, L. L. Lanier, J. C. Bigge, R. B. Parekh, et al. 1996. The inter-locus recombinant HLA-B\*4601 has high selectivity in peptide binding and functions characteristic of HLA-C. *J. Exp. Med.* 184:735.